Atmos. Chem. Phys. Discuss., 12, 18325–18377, 2012
www.atmos-chem-phys-discuss.net/12/18325/2012/
doi:10.5194/acpd-12-18325-2012

Atmospheric Chemistry and Physics Discussions

Global CFC-11 ($CFCl_3$) and CFC-12 (CF_2Cl_2) measurements with the Michelson Interferometer for Passive Atmospheric Sounding (MIPAS): retrieval, climatologies and trends

S. Kellmann[1], T. von Clarmann[1], G. P. Stiller[1], E. Eckert[1], N. Glatthor[1], M. Höpfner[1], M. Kiefer[1], J. Orphal[1], B. Funke[2], U. Grabowski[1], A. Linden[1], G. S. Dutton[3,4], and J. W. Elkins[3]

[1]Karlsruhe Institute of Technology (KIT), Institute for Meteorology and Climate Research (IMK), Karlsruhe, Germany
[2]Instituto de Astrofísica de Andalucía, CSIC, Granada, Spain
[3]NOAA Earth System Research Laboratory, Boulder, CO 80305, USA
[4]Cooperative Institute for Research in Environmental Sciences, University of Colorado, Boulder, CO 80309, USA

Received: 11 June 2012 – Accepted: 29 June 2012 – Published: 25 July 2012

Correspondence to: S. Kellmann (sylvia.kellmann@kit.edu)

Published by Copernicus Publications on behalf of the European Geosciences Union.

Abstract

Vertical profiles of CFC-11 ($CFCl_3$) and CFC-12 (CF_2Cl_2) have been measured with the Michelson Interferometer for Passive Atmospheric Sounding (MIPAS) with global coverage under daytime and nighttime conditions. The profile retrieval is based on constrained nonlinear least squares fitting of measured limb spectral radiance to modeled spectra. CFC-11 is measured in its ν_4-band at 850 cm^{-1}, and CFC-12 is analyzed in its ν_6-band at 922 cm^{-1}. To stabilize the retrievals, a Tikhonov-type smoothing constraint is applied. Main retrieval error sources are measurement noise and elevation pointing uncertainties. The estimated CFC-11 retrieval errors including noise and parameter errors but excluding spectroscopic data uncertainties are below 10 pptv in the middle stratosphere, depending on altitude, the MIPAS measurement mode and the actual atmospheric situation. For CFC-12 the total retrieval errors are below 28 pptv at an altitude resolution varying from 3 to 5 km. Time series of altitude/latitude bins were fitted by a simple parametric approach including constant and linear terms, a quasi-biennial oscillation (QBO) proxy and sine and cosine terms of several periods. In the time series from 2002 to 2011, quasi-biennial and annual oscillations are clearly visible. A decrease of stratospheric CFC mixing ratios in response to the Montreal Protocol is observed for most altitudes and latitudes. However, the trends differ from the trends measured in the troposphere, they are even positive at some latitudes and altitudes, and can in some cases only be explained by decadal changes in atmospheric age of air spectra or vertical mixing patterns.

1 Introduction

Prior to the reduced emissions in response to the Montreal Protocol signed in 1987, CFC-11 ($CFCl_3$) and CFC-12 (CF_2Cl_2) were the major sources of stratospheric chlorine. The stratospheric chlorine loading reached its maximum in 1996/1997, and a slow decline of stratospheric total chlorine has been observed since then

(Rinsland et al., 2003). Beyond being a source for reactive chlorine, which plays a major role in stratospheric ozone depletion (Molina and Rowland, 1974), the long lifetimes of these species (Ko and Sze, 1982) make them ideal tracers for dynamic processes such as subsidence (e.g. Toon et al., 1992), horizontal transport, and mixing (e.g. Waugh et al., 1997).

Recently, evidence has been found that the lifetimes of CFC-11 and CFC-12 might have been underestimated, and their reevaluation is considered a high priority action in atmospheric sciences, because of their role as a source of ozone destructing substances (Ko et al., 2011). A necessary prerequisite for a reassessment of lifetime of these CFCs are stratospheric measurements.

Atmospheric chlorofluorocarbon (CFC) abundances are measured since the early 1970s (Lovelock, 1971). A variety of in-situ and remote sensing techniques has been developed for this purpose in the following years, see, e.g. the bibliography in Goldman et al. (1976). Stratospheric CFC abundances are typically measured by air sampling techniques and subsequent laboratory analysis (e.g. Lueb et al., 1975; Heidt et al., 1975; Engel et al., 1998), by in-situ techniques (e.g. Robinson et al., 1977; Bujok et al., 2001; Romashkin et al., 2001), or remotely by infrared spectroscopy from balloon-borne (e.g. Murcray et al., 1975; Williams et al., 1976) or space-borne (e.g. Zander et al., 1987) platforms in solar occultation geometry. More recent solar occultation instruments used for CFC-detection include the Improved Limb Atmospheric Spectrometer (ILAS) (Khosrawi et al., 2004) and the Atmospheric Chemistry Experiment (ACE) (Mahieu et al., 2008; Brown et al., 2011).

Independently of a solar background signal, CFCs can also be measured by limb emission spectroscopy, as first documented by Brasunas et al. (1986) and Kunde et al. (1987). Space-borne limb emission measurements of CFCs were reported by Roche et al. (1993) for the Cryogenic Limb Array Etalon Spectrometer (CLAES, Bingham et al., 1997) for the Cryogenic Infrared Radiance Instrumentation for Shuttle (CIRRIS 1A), and by Spang et al. (1997) for the Cryogenic IR spectrometers and Telescopes (CRISTA). This series of space-borne limb-emission CFC-measurements has

been continued with the Michelson Interferometer for Passive Atmospheric Sounding (MIPAS) (Höpfner et al., 2007; Hoffmann et al., 2008). In this paper, we present the retrieval of CFC-11 and CFC-12 volume mixing ratio (VMR) profiles from limb emission spectra and report on the climatology and trends of retrieved profiles. These climatologies have been prepared as a contribution to the SPARC (Stratospheric Processes and their Role in Climate) data initiative (Hegglin and Tegtmeier, 2011).

2 MIPAS data

MIPAS is a cryogenic limb emission Fourier transform spectrometer designed for measurement of trace species from space (Endemann and Fischer, 1993; European Space Agency, 2000; Endemann et al., 1996; Fischer and Oelhaf, 1996; Fischer et al., 2008). It is part of the instrumentation of the Environmental Satellite (ENVISAT) which was launched into a sun-synchronous polar orbit on 1 March 2002. MIPAS was operated from July 2002 to March 2004 with full spectral resolution (FR) specification (0.05 cm^{-1} in terms of full width at half maximum, after apodization with the "strong" Norton and Beer (1976) function, corresponding to a maximum optical path difference of 20 cm). After a failure of one of the interferometer slide, MIPAS was operating from January 2005 on in the reduced spectral resolution (RR) mode (0.121 cm^{-1}) with an optical path difference of 8.0 cm. We consider MIPAS measurements in the so-called nominal mode, see Table 1. Data presented here were recorded from July 2002 to April 2011, which equates to about 2 million profiles for CFC-11 and CFC-12. The data analysis reported in this paper relies on the ESA-provided so-called level-1B data product which includes calibrated phase-corrected and geolocated radiance spectra (Nett et al., 1999), ESA data versions MIPAS/4.61 to MIPAS/4.62 for measurements recorded from 2002 to 2004, and MIPAS/5.02 to MIPAS/5.06 for measurements recorded since 2005. All spectra under consideration here were measured according to the standard measurement scenarios with nominal tangent altitudes from the upper troposphere to the mesosphere. Table 1 lists the scan sequences for MIPAS FR (July 2002–March 2004)

and RR (since 2005) nominal measurement modes (Dudhia, 2012). Data versions presented in this paper are V3O_CFC11_10 and V3O_CFC12_10 for FR measurements and V5R_CFC11_220 and V5R_CFC12_220 for RR measurements. Version 6 of the operational ESA data product, just recently released, also includes CFC-11 and CFC-12. Besides data presented in this study, there exist also MIPAS CFC data retrieved by distinct data analysis schemes (Dinelli et al., 2010; Hoffmann and Riese, 2004; Hoffmann et al., 2008; Moore et al., 2004; Dudhia, 2012).

3 CFC Retrievals

The retrieval of CFC-11 and CFC-12 profiles presented here was performed with a MIPAS data processor dedicated for scientific applications, which has been developed at the Institute for Meteorology and Climate Research (IMK) and complemented by components relevant to treatment of non-local thermodynamic equilibrium (non-LTE; not used in this study since not relevant to retrieval of CFCs) at the Instituto de Astrofísica de Andalucía (IAA). The general strategy of the IMK/IAA data processing has been documented in von Clarmann et al. (2003b). It underwent a pre-flight functionality study and validation by cross-comparison with various other data-processors within the framework of a blind test retrieval study von Clarmann et al. (2003a).

CFC-11 and CFC-12 are retrieved by constrained multi-parameter non-linear least squares fitting of modeled to measured spectra. Spectral data from all tangent altitudes are analyzed within one inversion process, as suggested by Carlotti (1988). VMR vertical profiles are retrieved on a fixed, i.e. tangent altitude independent height grid which is finer than the tangent altitude spacing (50 retrieval altitudes for CFC-11: 1-km steps from 4 to 45 km, then 5-km gridwidth to 50 km, 10-km steps from 60 to 100 km, and 20-km step to 120 km. 60 retrieval altitudes for CFC-12: 1-km steps from 4 to 44 km, then 2-km gridwidth from 46 to 70 km, 5-km steps from 75 to 80 km, and 10-km steps from 90 to 120 km). The horizontal spacing is 510 km for the FR resolution data nominal mode and 410 km for the RR nominal mode. In order to obtain stable profiles,

the profiles have been constrained such that the first order finite difference quotient ΔVMR/Δaltitude at adjacent altitude gridpoints was minimized, using the formalism as proposed by Tikhonov (1963). For both trace gases we use a zero a priori profile. The strength of the regularization has been chosen altitude-dependent with a scheme proposed by Steck (2002).

Forward modeling of spectra is performed with the Karlsruhe Optimized and Precise Radiative Transfer Algorithm (KOPRA) (Stiller, 2000; Stiller et al., 2002) using a dedicated spectroscopic database for MIPAS compiled by Flaud et al. (2003). CFC-11 and CFC-12 bands were modeled by 2-dimensional interpolation of pressure-, temperature-, and wavenumber-resolved laboratory measurements (Varanasi, 1992; Varanasi and Nemtchinov, 1994) to the actual atmospheric pressures and temperatures. The spectroscopic uncertainty of this data has been estimated in the literature to 5 % (Rothman et al., 1998; Rinsland et al., 2005), however the spectral resolution (0.03 cm^{-1} and 0.01 cm^{-1} at pressures below 40 Torr) of the laboratory data may introduce small systematic errors, together with the interpolation to different temperatures and pressures. Indeed, CFC-11 and CFC-12 show dense and sharp spectral structure at very high spectral resolution, even in the Q-branches (see, e.g. Orphal, 1991; McNaughton et al., 1994, 1995; D'Amico et al., 2002). It is also important to note that comparisons of the absolute band intensities (see, e.g. Varanasi and Nemtchinov, 1994; D'Amico et al., 2002) with other studies show larger differences. For these reasons, the absolute uncertainty of the spectroscopic data is estimated to 10 %, in the absence of further information.

Local spherical homogeneity of the atmosphere is assumed here, i.e. atmospheric state parameters related to one limb sounding sequence are not allowed to vary with latitude or longitude but only with altitude. The only exception is temperature: for data versions V5R_CFC11_220 and V5R_CFC12_220, a horizontal temperature gradient, calculated from ECMWF temperature fields, was taken into consideration in a range of ±400 km around the tangent point to reduce related retrieval artefacts (Kiefer et al., 2010).

Prior to trace gas retrievals, a spectral shift correction is applied first. Then elevation pointing correction and the temperature retrieval are performed (von Clarmann et al., 2003b, 2009b), and results are used in the subsequent trace gas retrievals. The most recent CFC data versions (V5R_CFC11_220 and V5R_CFC12_220) are based on a temperature and pointing retrieval where ozone and water vapor are jointly retrieved. This reduces the dependence of related a priori information on these species and related error propagation. Older data versions (V4O) where information on O_3 and H_2O was taken from climatologies during the temperature and elevation pointing retrieval led to temperature artifacts at about 30° N/S where the climatology was switched from the tropical to the mid-latitudinal case. These artifacts propagated onto the species retrievals and led to rabbit-ears-like structures in the altitude/latitude cross-sections of tropospheric source gases, which are no longer found in the V5R_CFC11_220 and V5R_CFC12_220 data. After temperature and line of sight (LOS) retrieval, the next steps are dedicated H_2O and O_3 retrievals, of which the results were found superior over the results of the joint retrieval of temperature, elevation pointing, ozone, and water vapor. After that, species abundances are retrieved in the order HNO_3, CH_4 together with N_2O, $ClONO_2$, N_2O_5, ClO, and finally CFC-11 and CFC-12. Each gas is retrieved in its specific spectral region, where results from preceding species abundance retrievals are used as input for the next species retrieval.

3.1 CFC-11

CFC-11 was analyzed in the 831.0–853.0 cm^{-1} spectral region, which covers the main part of the ν_4 band. Main interfering species in this region are H_2O, the HNO_3 ν_5 band, and the $COCl_2$ ν_5 band (Toon et al., 2001). In order to avoid propagation of uncertainties of a priori knowledge on these species to the CFC-11 profiles, their abundances were jointly fitted along with CFC-11 in this analysis window. Although H_2O results are available from preceding retrievals, joint-fitting led to reduced residuals in the H_2O lines, most probably due to inconsistencies between spectroscopic data in the H_2O analysis windows and the CFC-11 analysis window. Furthermore, a background-dependent

continuum signal and a zero-radiance calibration correction were determined along with the species abundances, as discussed in von Clarmann et al. (2003b). At tangent heights above 40 km CFC-11 is far below the detection limit. Thus, to save computing time, we used the twelve lowermost tangent heights, which correspond to altitudes between 5 km and 38 km for the FR data, and the nineteen lowermost tangent heights, which cover the 5 km and 40 km altitude range for the RR data.

Retrieval error estimates for sample FR and RR CFC-11 retrievals are shown in Tables 2 and 3, respectively. The high resolution measurement was taken at high southern latitudes on 21 May 2003. The estimated total retrieval error is 6.4 pptv at 25 km and 45.0 pptv at 10 km altitude. The RR measurement was taken in northern mid-latitudes on 19 September 2009. The related estimated total retrieval error is 6.1 pptv at 25 km and 19.0 pptv at 10 km altitude. For both measurement modes, the total retrieval error in the middle stratosphere (above 15–20 km) is dominated by measurement noise, while in the troposphere and lower stratosphere the leading error sources are uncertainties in elevation pointing (line of sight error), uncertainties in the abundances of the peroxyacetyl nitrate (PAN), NH_3, and OCS abundances, as well as spectral calibration uncertainties (gain error) and temperature uncertainties.

Selected rows of the CFC-11 averaging kernel matrices for both measurement modes are shown in Fig. 1. The altitude resolution in terms of full width at half maximum of a row of the averaging kernel matrix is about 4 km for the FR measurements, and about 2 to 3 km for the RR measurements. The averaging kernels are well-behaved in a sense that they peak at their nominal altitudes between about 6 km and 25 km for high spectral resolution and between about 10 and 25 km for RR measurements. Below and above, the retrievals are particularly sensitive to the real atmosphere below the nominal altitude. This is because the retrieval is strongly regularized to cope with the low sensitivity at these altitudes. The retrieved CFC-11 profiles represent approximately 4 to 7 degrees of freedom for the FR measurements and 5 to 9 degrees of freedom for the RR measurements, respectively. The better vertical resolution in the RR data is caused by finer vertical sampling.

The horizontal information smearing (we intentionally avoid the term "horizontal resolution" because the resolution can never be better than the horizontal sampling) was estimated on the basis of 2-D averaging kernels, evaluated on the basis of 2-D Jacobians of 1-D retrievals as described in von Clarmann et al. (2009a). The horizontal information smearing of a MIPAS retrieval in terms of full width at half maximum of the horizontal component of the 2-D averaging kernel is approximately 200–500 km, depending on measurement mode and altitude (Table 4). In many cases, the smearing is smaller than the horizontal sampling, implying that the horizontal resolution is limited by the horizontal sampling grid rather than the horizontal information smearing.

The information displacement is the horizontal distance between the point where most information comes from and the nominal geolocation of the limb scan, which is defined as the geolocation of the tangent point of the middle line of sight in a MIPAS limb scan. Compared to the nominal geolocation, the tangent points are displaced towards the satellite for the lowermost tangent altitude and in the opposite direction for the uppermost tangent altitude. This displacement is caused by the satellite movement and the position of the tangent point as a function of the elevation angle. Beyond this, also atmospheric opacity and regularization of the retrievals contribute to the information displacement. In Table 5 the CFC-11 weighted displacements are listed for altitudes of interest. Negative distances are displacements towards beyond the tangent point, positive distances are displacements towards the satellite. Except for higher altitudes the displacements are small compared to the horizontal sampling distance.

Figure 2 shows examples of a measured versus best fit modeled CFC-11 spectra, along with related residual spectra. For the FR measurement, a spectrum recorded at about 14 km tangent altitude is shown, which was measured on 21 May 2003. The broad spectral signature of CFC-11 is well reproduced. The root mean square (rms) of the residual is 16.91 $nW/(cm^2\,sr\,cm^{-1})$ which is about equal to the nominal noise equivalent spectral radiance (NESR) in the wavenumber region 830–850 cm^{-1}, which is 15 $nW/(cm^2\,sr\,cm^{-1})$ for apodized spectra. The RR spectrum was recorded at about 14 km tangent altitude on 19 September 2009. Also this spectrum is well reproduced

and the rms of the residual is 12.78 nW/(cm^2 sr cm^{-1}), which also is about equal to the nominal apodized noise equivalent spectral radiance of 12 nW/(cm^2 sr cm^{-1}).

3.2 CFC-12

CFC-12 was analyzed in the 915.0–925.0 cm^{-1} spectral region, which covers the central part of the ν_6 band. Main interfering signals are caused by the CO_2 10001 ← 00011 so-called laser band, the HNO_3 $2\nu_9$ band, H_2O and a weak PAN band. All these interfering species were jointly fitted along with continuum and offset-correction. In contrast to CFC-11 we used all available tangent heights for the CFC-12 retrieval, because the measurable signal of CFC-12 extends to higher altitudes than that of CFC-11.

Error estimates for CFC-12 FR and RR measurements are shown in Table 6 and Table 7, respectively. The estimated total retrieval error of CFC-12 retrieved from high spectral resolution measurements is 20.0 pptv for 25 km and 18.0 pptv for 10 km altitude. At 20 km and above measurement noise is the leading error source, while below parameter errors are dominating. The main parameter error components are the line of sight elevation pointing error, gain calibration error, the error of the horizontal (along track) temperature gradient, the temperature error itself, and the uncertainty in the NH_3 profile. For RR CFC-12 retrievals, the relative importance of the various error sources is similar, except that the horizontal temperature inhomogeneities do not appear as error source since horizontal temperature gradients were accounted for in the retrieval. In the stratosphere, total retrieval errors are only slightly larger than for high spectral resolution measurements (22.0 pptv at 25 km) but at 10 km the error is much larger (64.0 pptv) because of propagated parameter uncertainties, for the example chosen.

The altitude resolution in terms of full width at half maximum of a row of the averaging kernel matrix is about 3 to 5 km for the FR measurements and about 3 to 4 km for the RR measurements. This corresponds to 6–9 degrees of freedom for FR measurements and 9–13 for RR measurements. CFC-12 averaging kernels are shown in Fig. 3. They are well-behaved between about 8 and 40 km for high spectral retrievals and between

10 and 50 km for RR measurements. As for CFC-11, the better altitude resolution of the RR measurements is due to the better vertical sampling.

Figure 4 shows examples of measured (black) versus fitted (red) CFC-12 spectra. The high spectral resolution measurement was recorded on 21 May 2003 at the border of the southern polar cap and the tangent altitude is 11 km. The measured spectrum is well reproduced and the rms of the residual is 19.15 nW/(cm^2 sr cm^{-1}) which is slightly higher than the nominal noise equivalent spectral radiance. The RR was recorded on 19 September 2009 at a tangent altitude of 11 km. Here the rms of the fit residual (13.84 nW/(cm^2 sr cm^{-1})) is even slightly less than the nominal noise equivalent spectral radiance.

The horizontal information smearing of CFC-12 retrievals is approximately 300 km at altitudes below 24 km and more than 400 km above for the FR retrievals (Table 8). For the RR retrievals assessed here, it is between about 300 km and more than 500 km. As for CFC-11, the information displacement is clearly smaller than the horizontal measurement grid (Table 9).

4 The SPARC climatologies

MIPAS CFC climatologies have been prepared in compliance with the methodical and data format requirements of the SPARC (Stratospheric Processes and their Role in Climate) data initiative (Hegglin and Tegtmeier, 2011). The climatology consists of zonal monthly mean fields of CFC volume mixing ratios on 28 pressure levels of 300, 250, 200, 170, 150, 130, 115, 100, 90, 80, 70, 50, 30, 20, 15, 10, 7, 5, 3, 2, 1.5, 1.0, 0.7, 0.5, 0.3, 0.2, 0.15, 0.1 hPa. Along with these monthly means, standard deviations and sample sizes are provided. Technical details of the generation of this climatologies follow the approach published by von Clarmann et al. (2012).

4.1 CFC-11 observations

Figure 5 shows monthly zonal means of CFC-11 between 200 hPa and 10 hPa for September 2002, December 2003, March 2008, and June 2010. Largest mixing ratios are seen in the tropics in the upwelling branch of the Brewer-Dobson circulation. With increasing altitude and latitude mixing ratios become smaller, reflecting photochemical and OH-driven CFC-depletion in aged air. The decrease of CFC-11 from the years 2002 to 2010 is noticeable particularly in the tropical tropopause, where the air is youngest. Here the effect of reduced CFC emissions in response to the Montreal Protocol is best visible.

Figures 6 and 7 illustrate the temporal evolution of CFC-11 for all latitudes between July 2002 and April 2011 at selected altitude levels from 200 hPa to 15 hPa. Between April and December 2004 no MIPAS data are available because of the instrument failure mentioned in Sect. 2. Particularly at 200 hPa there is an obvious bias between the FR and the RR data, mainly caused by the improved vertical resolution of the latter. Nevertheless, the decadal decrease of CFC-11 is well observable in these time series at all altitudes over the entire measuring period. Furthermore, the annual cycle is clearly visible, and it is in opposite phase in the Southern versus the Northern Hemisphere, following the local season. In the stratosphere, minimum mixing ratios are found in the polar winter, due to the subsidence of old air depleted of CFCs. In the troposphere, there is a polar summer minimum, in consistence with the seasonal cycle seen in in-situ and flask data published by Butler et al. (1998). All time series show, as expected, the maxima of the CFC-11 volume mixing ratios in the tropical and subtropical zone between 30° S to 30° N. The region of large CFC-11 amounts, however, is not symmetrical around the equator but shifted by a couple of degrees to northern latitudes. The stratospheric mixing barrier, discernable by the region of the largest CFC-11 zonal gradient at 15 hPa, 20 hPa, 50 hPa, and 70 hPa varies with season between 20°, 25°, 30° and 40° in the Northern Hemisphere, compared to 12°, 15°, 20° and 30° in the Southern Hemisphere. A difference between hemispheres was also found by

Palazzi et al. (2011). At 15 hPa, 20 hPa and 50 hPa a clear signal of the quasi-biennial oscillation (QBO) is visible.

4.2 CFC-12 observations

Figure 8 shows monthly zonal mean CFC-12 mixing ratio distributions between 200 hPa and 1 hPa of CFC-12 in September 2002, December 2003, March 2008, and June 2010. The structures are similar to those of CFC-11 but the CFC-12 survives the transport into higher altitudes in the ascending branch of the Brewer-Dobson circulation, because it is more stable under sunlit conditions. Also for CFC-12 a decrease with time is observable, but it is much less pronounced than that of CFC-11. This is because the decomposition of CFC-12 in the atmosphere is slower than that of CFC-11. The lifetime of CFC-12 in the stratosphere of about 100 yr is larger than that of CFC-11 which is about 45 yr (Cunnold et al., 1997; Volk et al., 1997). Time series (Figs. 9 and 10) show basically the same features already discussed for CFC-11 (negative trend, annual cycle, QBO, and asymmetry around the equator). Also for CFC-12 there is a bias between FR and RR measurements, most pronounced at lower altitudes.

5 Trends

5.1 Method

Time series of monthly mean CFC-11 and CFC-12 mixing ratios at selected altitudes and for 10° latitude bins have been analyzed by fitting the following regression function to the data (Stiller et al., 2012)

$$\mathrm{VMR}(t) = a + bt + c_1 \mathrm{qbo}_1(t) + d_1 \mathrm{qbo}_2(t) + \\ + \sum_{n=2}^{9} \left(c_n \sin \frac{2\pi t}{l_n} + d_n \cos \frac{2\pi t}{l_n}\right) \quad (1)$$

where t is time, qbo_1 and qbo_2 are quasi-biennial oscillation (QBO) indices. The terms under the sum are 8 sine and cosine functions of the period length l_n, which represent the seasonal and the semi-annual cycle and their "overtones" with period lengths of 3, 4, 8, 9, 18, and 24 months. Sine and cosine of the same period length are both fitted to account for any phase shift of the variation. The terms qbo_1 and qbo_2 are the normalized Singapore winds at 30 hPa and 50 hPa. These are provided by the Free University of Berlin via http://www.geo.fu-berlin.de/met/ag/strat/produkte/qbo/index.html. As suggested by Kyrölä et al. (2010), we exploit the approximate orthogonality of qbo_1 and qbo_2 to emulate any QBO phase shift by their combination with different weights. Coefficients a, b, c_1, ..., c_9, d_1, ..., d_9 are fitted to the data using the method of von Clarmann et al. (2010), where the full error covariance matrix of mixing ratios is considered, with the squared standard errors of the monthly means as the diagonal terms. In a first step of the analysis, covariances are only important to consider any bias between the FR and the RR CFC measurements due to the change of the MIPAS measurement modes. Since these biases are thought to be primarily caused by different altitudes resolutions, they can depend on altitude and latitude. For each time series at a certain altitude and latitude band, the bias can simply be treated as a fully correlated error component of one of both data subsets. This method is very robust with respect to the estimate of the residual bias used to create the covariance matrix. Consideration of the bias in the covariance matrix has been shown to be equivalent to the inference of the bias from the data themselves with an optimal estimation scheme where the a priori variance of the residual bias equals the residual bias component in our covariance matrix (cf. von Clarmann et al., 2001). From the fit residuals, additional autocorrelated error terms are estimated and added to the initial covariances, as described by Stiller et al. (2012). A second trend fit is performed with the enhanced covariance matrix, which is then used for the scientific analysis.

5.2 Results for CFC-11

Trends of CFC-11 based on monthly zonal mean mixing ratios in 10° latitude bins have been calculated for selected altitudes. Data coverage was good from July 2002 to March 2004 with measurements available for about 16 to 31 days per month. From 2005 to 2007 data coverage was quite inhomogeneous when the number of days for which nominal mode measurements were available varied from 2 to 30 days per month, while since then MIPAS has again been operated at full duty cycle and nearly continuous coverage. Figure 11 shows examples of measured and best fitting time series. A negative trend is obvious in all these examples, as well as the annual variation, and the bias between the data subsets V3O_CFC11_10 and V5R_CFC11_220. The minima of mid-latitudinal measurements occur in local winter (left panels). The amplitude of the annual cycle is largest at polar latitudes. In the tropical time series a clear QBO signal is visible (upper right panel), while the amplitude of the annual cycle is largely reduced compared to higher latitudes.

Liang et al. (2008) report northern and southern hemispheric averaged monthly mean surface CFC-11 and CFC-12 mixing ratios between January 1977 and December 2004 based on measurements of different long-term observations (Prinn et al., 2000; Montzka et al., 1999; Thompson et al., 2004). Their CFC-11 monthly mean values in the year 2002 are about 260 pptv which coincides well with the starting point of our regression line with mixing ratios between 260 to 265 pptv at ∼10 km altitude. CFC-11 measurements are also provided by the Halocarbons and other Atmospheric Trace Species (HATS) group at NOAA/ESRL (Elkins et al., 2012a). They provide a combined data set from various NOAA/ESRL measurement programs; the method for combining the various NOAA/ESRL measurement programs into one data set is described by Hall et al. (2011). These CFC-11 measurements for April 2011 are about 240 pptv which agrees very well with our values between 229 and 242 ppt at 10 km altitude (Fig. 11, right middle panel, left and right lower panel).

The inferred trends from 2002–2011 for all latitude/altitude bins are summarized in Fig. 12, along with estimated 1-sigma uncertainties and significance of the trends in terms of multiples of sigma. The estimated uncertainties include the additional auto-correlated error term discussed in Sect. 5.1 and are consistent with the fit residuals in a sense that the reduced χ^2 values are close to unity. In wide parts of the atmosphere highly significant negative trends between −10 and −40 pptv per decade are found. These trends agree well with the tropospheric trends of about −25 pptv per decade in the same period measured by the HATS group (Elkins et al., 2012a) and the data reported by Butler et al. (1998) (−23 pptv per decade), of which the extension to current dates can be found on http://www.esrl.noaa.gov/gmd/hats/graphs/graphs.html. Differences between the MIPAS percentage trends and the age-corrected tropospheric trends are shown in Fig. 13. Age of air has been taken from Stiller et al. (2012). We would like to stress that we do not necessarily expect the stratospheric trends to reproduce the tropospheric ones with a time lag depending on the age of stratospheric air, because stratospheric circulation is supposed to change, affecting the time lag and possibly the level of depletion of the air observed. For an atmosphere without changes in stratospheric dynamics and delta-shaped age spectra, the differences shown in Fig. 13 are expected to be zero throughout. However we find positive and negative trend differences of several ten percent. The positive trend values between 10° S–90° S in the stratosphere between about 22 km and 30 km altitude can be explained by air with broad age spectra, containing particularly old air which has entered the stratosphere prior to about 1993 when tropospheric CFC-11 concentrations reached their maximum. The mean age alone, which is about 5 yr in this altitude/latitude-range (Stiller et al., 2012) cannot explain the positive trend. In the upper northern hemispheric stratosphere, trends are more negative than expected from the tropospheric trends corrected for the age of air. This is the region where Stiller et al. (2012) have found a pronounced increase in the age of stratospheric air, which, however, cannot alone explain the larger negative trends. Instead, changing circulation and/or mixing patterns which heavily affect the shape of the age spectra may be able to explain both, the increase of age of

air and the stronger negative CFC-11 trends. However, a fully consistent explanation is not yet available.

5.3 Results for CFC-12

The findings on periodic and quasi-periodic variations of CFC-11 also apply to CFC-12 (Fig. 14). The annual variation and the QBO are well represented by the regression model. In comparison to the CFC-12 mixing ratios of ∼543 pptv as reported by Liang et al. (2008) for the year 2002 our values at the starting point of the regression line in 2002 are slightly lower with mixing ratios between 524 and 537 pptv. The HATS group reports mixing ratios for a CFC-12 data set combined from various NOAA/ESRL measurement programs of about 528 pptv for April 2011 (Elkins et al., 2012b), which is slightly higher than the MIPAS data at the end of the regression line where mixing ratios vary with latitude between 506 and 508 pptv (Fig. 14, right middle panel, left and right lower panel).

A survey of the inferred trends is given in Fig. 15. The patterns of positive and negative trends of CFC-12 are similar to those of CFC-11 but are better visible. In the troposphere and in the lower stratosphere where relatively young air is observed consistently (Stiller et al., 2012), the trends are negative throughout, with typical values around −20 pptv per decade, which again is in agreement with tropospheric trend measurements by Elkins et al. (2012a) and the extension of the record by Butler et al. (1998). Particularly large negative trends are observed in the middle northern hemispheric stratosphere, with largest negative values at 20° N–30° N, 25 km altitude. Similar to CFC-11, these negative trends are larger than the age corrected tropospheric trends (Fig. 16), and occur again in the region where Stiller et al. (2012) found the increase in mean age of air. Similar to CFC-11, we suggest that changing circulation and/or mixing patterns affect the shape of age spectra and may lead to steepening of the trends relative to the tropospheric ones. Above this region (above 20–30 km altitude at latitudes from 90° N–20° N, respectively), slightly positive trends have been found. With an age of approximately 6 yr, the starting point of the time series (2002)

refers to tropospheric air in 1996, when CFC-12 still increased. For the positive trends in the middle southern hemispheric stratosphere the same explanation as for CFC-11 applies. The effect is, however, more pronounced for CFC-12, because its tropospheric maximum was reached later. Of course there are also other possible explanations for differences between stratospheric and tropospheric CFC-trends, e.g. decadal variations of subsidence or mixing of CFC-depleted air from higher altitudes. All plausible explanations, however, imply decadal changes in stratospheric dynamics.

6 Conclusions

Global altitude-resolved zonal mean distributions of stratospheric CFC-11 and CFC-12 were inferred from MIPAS measurements. Altitude- and latitude resolved time series show the expected annual cycle (strongest at high latitudes) and QBO signal (strongest in the tropics). As expected as response to the Montreal Protocol, at most altitudes and latitudes negative trends are observed, which are on average consistent to the trends of tropospheric CFC-11 and CFC-12 mixing ratios. However, the CFC trends in the stratosphere vary with altitude and latitude, and in some regions even positive trends are observed. Generally speaking, trends are mostly negative where age trends as reported by Stiller et al. (2012) are positive and vice versa, but this picture is not fully consistent. All plausible explanations for the observed CFC-trends involve some kind of decadal change in stratospheric dynamics. Either substantial changes in the shape of the age spectra or changes in vertical mixing patterns are needed to solve the apparent contradiction. The use of these MIPAS CFC-measurements for a quantitative analysis of stratospheric age-of-air spectra under consideration of their altitude and latitude dependent lifetimes will be a major focus for our research in the next years.

Acknowledgements. ESA has provided MIPAS Level-1B data. Meteorological analysis data have been provided by ECMWF. Development of CFC-11 and CFC-12 data retrieval was partly funded by the German Federal Ministry of Education and Research (BMBF) under contract no. 50EE0901.

The service charges for this open access publication have been covered by a Research Centre of the Helmholtz Association.

References

Bingham, G. E., Zhou, D. K., Bartschi, B. Y., Anderson, G. P., Smith, D. R., Chetwynd, J. H., and Nadile, R. M.: Cryogenic Infrared Radiance Instrumentation for Shuttle (CIRRIS 1A) Earth limb spectral measurements, calibration, and atmospheric O_3, HNO_3, CFC-12, and CFC-11 profile retrieval, J. Geophys. Res., 102, 3547–3558, 1997. 18328

Brasunas, J. C., Kunde, V. G., Hanel, R. A., Walser, D., Herath, L. W., Buijs, H. L., Bérubé, J. N., and McKinnon, J.: Balloon-borne cryogenic spectrometer for measurement of lower stratospheric trace constituents, in: Proc. SPIE, Vol. 619, SPIE, Bellingham, WA, USA, 80–88, 1986. 18328

Brown, A. T., Chipperfield, M. P., Boone, C., Wilson, C., Walker, K. A., and Bernath, P. F.: Trends in atmospheric halogen containing gases since 2004, J. Quant. Spectrosc. Radiat. Transfer, 112, 2552–2566, doi:10.1016/j.jqsrt.2011.07.005, 2011. 18328

Bujok, O., Tan, V., Klein, E., Nopper, R., Bauer, R., Engel, A., Gerhards, M.-T., Afchine, A., McKenna, D. S., Schmidt, U., Wienhold, F. G., and Fischer, H.: GHOST – a novel airborne gas chromatograph for in situ measurements of long-lived tracers in the lower stratosphere: method and applications, J. Atmos. Chem., 39, 37–64, 2001. 18328

Butler, J. H., Montzka, S. A., Clarke, A. D., Lobert, J. M., and Elkins, J. W.: Growth and distribution of halons in the atmosphere, J. Geophys. Res., 103, 1503–1511, 1998. 18337, 18341, 18342

Carlotti, M.: Global-fit approach to the analysis of limb-scanning atmospheric measurements, Appl. Opt., 27, 3250–3254, 1988. 18330

Cunnold, D. M., Weiss, R. F., Prinn, R. G., Hartley, D., Simmonds, P. G., Fraser, P. J., Miller, B., Alyea, F. N., and Porter, L.: GAGE/AGAGE measurements indicating reductions in global emissions of CCl_3F and CCl_2F_2 in 1992–1994, J. Geophys. Res., 102, 1259–1269, 1997. 18338

D'Amico, G., Snels, M., Hollenstein, H., and Quack, M.: Analysis of the $\nu_3 + \nu_7$ combination band of CF_2Cl_2 from spectra obtained by high resolution diode laser and FTIR supersonic jet techniques, Phys. Chem. Chem. Phys., 4, 1531–1536, doi:10.1039/B110919G, 2002. 18331

Dinelli, B. M., Arnone, E., Brizzi, G., Carlotti, M., Castelli, E., Magnani, L., Papandrea, E., Prevedelli, M., and Ridolfi, M.: The MIPAS2D database of MIPAS/ENVISAT measurements retrieved with a multi-target 2-dimensional tomographic approach, Atmos. Meas. Tech., 3, 355–374, doi:10.5194/amt-3-355-2010, 2010. 18330

Dudhia, A.: http://www.atm.ox.ac.uk/group/mipas/rrmodes.html (last access: 16 July 2012), 2012. 18330, 18353

Elkins, J. W., Montzka, S. A., Hall, B., and Dutton, G.: Combined Chloroflurocarbon-11 data from the NOAA/ESRL global monitoring division, http://www.esrl.noaa.gov/gmd/hats/combined/CFC11.html, National Oceanic & Atmospheric Administration, Earth System Research Laboratory, Global Monitoring Division, Dep. of Commer., Boulder, CO, USA, 2012a. 18340, 18341, 18342

Elkins, J. W., Montzka, S. A., Hall, B., and Dutton, G.: Combined Chloroflurocarbon-12 data from the NOAA/ESRL global monitoring division, http://www.esrl.noaa.gov/gmd/hats/combined/CFC12.html, National Oceanic & Atmospheric Administration, Earth System Research Laboratory, Global Monitoring Division, Dep. of Commer., Boulder, CO, USA, 2012b. 18342

Endemann, M. and Fischer, H.: Envisat's high-resolution limb sounder: MIPAS, ESA Bull., 76, 47–52, 1993. 18329

Endemann, M., Gare, P., Smith, D., Hoerning, K., Fladt, B., and Gessner, R.: MIPAS design overview and current development status, in: Proceedings EUROPTO series, Optics in Atmospheric Propagation, adaptive systems, and Lidar techniques for Remote Sensing, Taormina, Italy, 24–26 September, Vol. 2956, 124–135, 1996. 18329

Engel, A., Schmidt, U., and McKenna, D.: Stratospheric trends of CFC-12 over the past two decades: Recent observational evidence of declining growth rates, Geophys. Res. Lett., 25, 3319–3322, 1998. 18328

European Space Agency: Envisat, MIPAS An instrument for atmospheric chemistry and climate research, ESA Publications Division, ESTEC, P. O. Box 299, 2200 AG Noordwijk, The Netherlands, SP-1229, 2000. 18329

Fischer, H. and Oelhaf, H.: Remote sensing of vertical profiles of atmospheric trace constituents with MIPAS limb-emission spectrometers, Appl. Opt., 35, 2787–2796, 1996. 18329

Fischer, H., Birk, M., Blom, C., Carli, B., Carlotti, M., von Clarmann, T., Delbouille, L., Dudhia, A., Ehhalt, D., Endemann, M., Flaud, J. M., Gessner, R., Kleinert, A., Koopman, R., Langen, J., López-Puertas, M., Mosner, P., Nett, H., Oelhaf, H., Perron, G., Remedios, J., Ridolfi, M., Stiller, G., and Zander, R.: MIPAS: an instrument for atmospheric and climate research, Atmos. Chem. Phys., 8, 2151–2188, doi:10.5194/acp-8-2151-2008, 2008. 18329

Flaud, J.-M., Piccolo, C., Carli, B., Perrin, A., Coudert, L. H., Teffo, J.-L., and Brown, L. R.: Molecular line parameters for the MIPAS (Michelson Interferometer for Passive Atmospheric Sounding) experiment, Atmos. Oceanic Opt., 16, 172–182, 2003. 18331

Goldman, A., Bonomo, F. S., and Murcray, D. G.: Statistical-band-model analysis and integrated intensity of the 10.8 µm band of CF_2Cl_2, Geophys. Res. Lett., 3, 309–312, 1976. 18328

Hall, B. D., Dutton, G. S., Mondeel, D. J., Nance, J. D., Rigby, M., Butler, J. H., Moore, F. L., Hurst, D. F., and Elkins, J. W.: Improving measurements of SF_6 for the study of atmospheric transport and emissions, Atmos. Meas. Tech., 4, 2441–2451, doi:10.5194/amt-4-2441-2011, 2011. 18340

Hegglin, M. and Tegtmeier, S.: The SPARC Data Initiative, SPARC Newslett., 36, 22–23, 2011. 18329, 18336

Heidt, L. E., Lueb, R., Pollock, W., and Ehhalt, D. H.: Stratospheric Profiles of CCl_3F and CCl_2F_2, Geophys. Res. Lett., 2, 445–447, doi:10.1029/GL002i010p00445, 1975. 18328

Hoffmann, L. and Riese, M.: Quantitative transport studies based on trace gas assimilation, Adv. Space Res., 33, 1068–1072, doi:10.1016/S0273-1177(03)00592-1, 2004. 18330

Hoffmann, L., Kaufmann, M., Spang, R., Müller, R., Remedios, J. J., Moore, D. P., Volk, C. M., von Clarmann, T., and Riese, M.: Envisat MIPAS measurements of CFC-11: retrieval, validation, and climatology, Atmos. Chem. Phys., 8, 3671–3688, doi:10.5194/acp-8-3671-2008, 2008. 18329, 18330

Höpfner, M., von Clarmann, T., Engelhardt, M., Fischer, H., Funke, B., Glatthor, N., Grabowski, U., Kellmann, S., Kiefer, M., Linden, A., López-Puertas, M., Milz, M., Steck, T., Stiller, G. P., Wang, D. Y., Ruhnke, R., Kouker, W., Reddmann, T., Bernath, P., Boone, C., and Walker, K. A.: Comparison between ACE-FTS and MIPAS IMK/IAA profiles of O_3, H_2O, N_2O, CH_4, CFC-11, CFC-12, HNO_3, $ClONO_2$, NO_2, N_2O_5, CO, and SF_6 in February/March 2004, in: Proc. Third Workshop on the Atmospheric Chemistry Validation of Envisat, (ACVE-3), 4–7 December, 2006, ESRIN, Frascati, Italy, vol. ESA SP-642, CD-ROM, ESA Publications Division, ESTEC, Postbus 299, 2200 AG Noordwijk, The Netherlands, 2007. 18329

Khosrawi, F., Müller, R., Irie, H., Engel, A., Toon, G. C., Sen, B., Aoki, S., Nakazawa, T., Traub, W. A., Jucks, K. W., Johnson, D. G., Oelhaf, H., Wetzel, G., Sugita, T., Kanzawa, H., Yokota, T., Nakajima, H., and Sasano, Y.: Validation of CFC-12 measurements from the Improved Limb Atmospheric Spectrometer (ILAS) with the version 6.0 retrieval algorithm, J. Geophys. Res., 109, D06311, doi:10.1029/2003JD004325, 2004. 18328

Kiefer, M., Arnone, E., Dudhia, A., Carlotti, M., Castelli, E., von Clarmann, T., Dinelli, B. M., Kleinert, A., Linden, A., Milz, M., Papandrea, E., and Stiller, G.: Impact of Temperature Field Inhomogeneities on the Retrieval of Atmospheric Species from MIPAS IR Limb Emission Spectra, Atmos. Meas. Tech., 3, 1487–1507, doi:10.5194/amt-3-1487-2010, 2010. 18331

Ko, M., Newman, P., Reinmann, S., and Strahan, S. E.: Lifetime of halogen source gases, available at: http://sparcclima.vs89.snowflakehosting.ch/activities/lifetime-halogen-gases/ (last access: 16 July 2012), 2011. 18328

Ko, M. K. W. and Sze, N. D.: A 2-D model calculation of atmospheric lifetimes for N_2O, CFC-11 and CFC-12, Nature, 297, 317–319, 1982. 18328

Kunde, V. G., Brasunas, J. C., Conrath, B. J., Hanel, R. A., Herman, J. R., Jennings, D. E., Maguire, W. C., Walser, D. W., Annen, J. N., Silverstein, M. J., Abbas, M. M., Herath, L. W., Buijs, H. L., Berube, H. L., and McKinnon, J.: Infrared spectroscopy of the lower stratosphere with a balloon- borne cryogenic Fourier spectrometer, Appl. Opt., 26, 545–553, 1987. 18328

Kyrölä, E., Tamminen, J., Sofieva, V., Bertaux, J. L., Hauchecorne, A., Dalaudier, F., Fussen, D., Vanhellemont, F., Fanton d'Andon, O., Barrot, G., Guirlet, M., Fehr, T., and Saavedra de Miguel, L.: GOMOS O_3, NO_2, and NO_3 observations in 2002–2008, Atmos. Chem. Phys., 10, 7723–7738, doi:10.5194/acp-10-7723-2010, 2010. 18339

Liang, Q., Stolarski, R. S., Douglass, A. R., Newman, P. A., and Nielsen, J. E.: Evaluation of emissions and transport of CFCs using surface observations and their seasonal cycles and the GEOS CCM simulation with emissions-based forcing, J. Geophys. Res., 113, D14302, doi:10.1029/2007JD009617, 2008. 18340, 18342

Lovelock, J. E.: Atmospheric fluorine compounds as indicators of air movements, Nature, 230, 379, doi:10.1038/230379a0, 1971. 18328

Lueb, R. A., Ehhalt, D. H., and Heidt, L. E.: Balloon-borne low temperature air sampler, Rev. Sci. Instr., 46, 702–705, 1975. 18328

Mahieu, E., Duchatelet, P., Demoulin, P., Walker, K. A., Dupuy, E., Froidevaux, L., Randall, C., Catoire, V., Strong, K., Boone, C. D., Bernath, P. F., Blavier, J.-F., Blumenstock, T., Coffey, M., De Mazière, M., Griffith, D., Hannigan, J., Hase, F., Jones, N., Jucks, K. W., Kagawa, A.,

Kasai, Y., Mebarki, Y., Mikuteit, S., Nassar, R., Notholt, J., Rinsland, C. P., Robert, C., Schrems, O., Senten, C., Smale, D., Taylor, J., Tétard, C., Toon, G. C., Warneke, T., Wood, S. W., Zander, R., and Servais, C.: Validation of ACE-FTS v2.2 measurements of HCl, HF, CCl_3F and CCl_2F_2 using space-, balloon- and ground-based instrument observations, Atmos. Chem. Phys., 8, 6199–6221, doi:10.5194/acp-8-6199-2008, 2008. 18328

McNaughton, D., McGilvery, D., and Robertson, E. G.: High-resolution FTIR-jet spectroscopy of CCl_2F_2, J. Chem. Soc., Faraday Trans., 90, 1055–1060, doi:10.1039/FT9949001055, 1994. 18331

McNaughton, D., McGilvery, D., and Robertson, E. G.: High resolution FTIR spectroscopy of CFC's in a supersonic jet expansion, J. Mol. Struct., 348, 1–4, 1995. 18331

Molina, M. J. and Rowland, F. S.: Stratospheric sink for chlorofluoromethanes: Chlorine atom-catalysed destruction of ozone, Nature, 249, 810–812, 1974. 18328

Montzka, S. A., Butler, J. H., Elkins, J. W., Thompson, T. M., Clarke, A. D., and Lock, L. T.: Present and future trends in the atmospheric burden of ozone-depletion halogens, Nature, 398, 690–694, 1999. 18340

Moore, D. P., Waterfall, A. M., Remedios, J. J., and Burgess, A.: Measuring Halocarbons with the MIPAS instrument, Geophys. Res. Abstr., 6, 04016, 2004. 18330

Murcray, D. G., Bonomo, F. S., Brooks, J. N., Goldman, A., Murcray, F. H., and Williams, W. J.: Detection of fluorocarbons in the stratosphere, Geophys. Res. Lett., 2, 109–112, 1975. 18328

Nett, H., Carli, B., Carlotti, M., Dudhia, A., Fischer, H., Flaud, J.-M., Perron, G., Raspollini, P., and Ridolfi, M.: MIPAS Ground Processor and Data Products, in: Proc. IEEE 1999 International Geoscience and Remote Sensing Symposium, 28 June–2 July 1999, Hamburg, Germany, 1692–1696, 1999. 18329

Norton, H. and Beer, R.: New apodizing functions for Fourier spectrometry, J. Opt. Soc. Am, 66, 259–264, (Errata J. Opt. Soc. Am., 67, 419,1977), 1976. 18329

Orphal, J.: Bestimmung von Linienparametern in der ν_8-Bande von CF_2Cl_2 (CFC-12) mittels hochauflösender Diodenlaserspektroskopie, Master's thesis, Humboldt-Universität zu Berlin, 1991. 18331

Palazzi, E., Fierli, F., Stiller, G. P., and Urban, J.: Probability density functions of long-lived tracer observations from satellite in the subtropical barrier region: data intercomparison, Atmos. Chem. Phys., 11, 10579–10598, doi:10.5194/acp-11-10579-2011, 2011. 18338

Prinn, R. G., Weiss, R. F., Fraser, P. J., Simmonds, P. G., Cunnold, D. M., Alyea, F. N., O'Doherty, S., Salameh, P., Miller, B. R., Huang, J., Wang, R. H. J., Hartley, D. E., Harth, C., Steele, L. P., Sturrock, G., Midgley, P. M., and McCulloch, A.: A history of chemically and radiatively important gases in air deduced from ALE/GAGE/AGAGE, J. Geophys. Res., 105, 17751–17792, doi:10.1029/2000JD900141, 2000. 18340

Rinsland, C. P., Mahieu, E., Zander, R., Jones, N. B., Chipperfield, M. P., Goldman, A., Anderson, J., Russell III, J. M., Demoulin, P., Notholt, J., Toon, G. C., Blavier, J.-F., Sen, B., Sussmann, R., Wood, S. W., Meier, A., Griffith, D. W. T., Chiou, L. S., Murcray, F. J., Stephen, T. M., Hase, F., Mikuteit, S., Schulz, A., and Blumenstock, T.: Long-term trends of inorganic chlorine from ground-based infrared solar spectra: Past increases and evidence for stabilization, J. Geophys. Res., 108, 4252, doi:10.1029/2002JD003001, 2003. 18328

Rinsland, C. P., Goldman, A., Mahieu, E., Zander, R., Chiou, L. S., Hannigan, J. W., Wood, S. W., and Elkins, J. W.: Long-term evolution in the tropospheric concentration of CCl_2F_2 (chlorofluorocarbon 12) derived from high spectral resolution infrared solar absorption spectra: retrieval and comparison with in situ surface measurements, J. Quant. Spectrosc. Radiat. Transfer, 92, 201–209, doi:10.1016/j.jqsrt.2004.07.022, 2005. 18331

Robinson, E., Rasmussen, R. A., Krasnec, J., Pierotti, D., and Jakubovic, M.: Halocarbon measurements in the Alaskan troposphere and lower stratosphere, Atmos. Environ., 11, 215–223, 1977. 18328

Roche, A. E., Kumer, J. B., Mergenthaler, J. L., Ely, G. A., Uplinger, W. G., Potter, J. F., James, T. C., and Sterritt, L. W.: The Cryogenic Limb Array Etalon Spectrometer CLAES on UARS: Experiment Description and Performance, J. Geophys. Res., 98, 10763–10775, 1993. 18328

Romashkin, P. A., Hurst, D. F., Elkins, J. W., Dutton, G. S., Fahey, D. W., Dunn, R. E., Moore, F. L., Myers, R. C., and Hall, B. D.: In situ measurements of long-lived trace gases in the lower stratosphere by gas chromatography, J. Atmos. Oceanic. Technol., 18, 1195–1204, 2001. 18328

Rothman, L. S., Rinsland, C. P., Goldman, A., Massie, T., Edwards, D. P., Flaud, J.-M., Perrin, A., Camy-Peyret, C., Dana, V., Mandin, J.-Y., Schroeder, J., McCann, A., Gamache, R. R., Wattson, R. B., Yoshino, K., Chance, K. V., Jucks, K. W., Brown, L. R., Nemtchinov, V., and Varanasi, P.: The HITRAN molecular spectroscopic database and HAWKS (HITRAN Atmospheric Workstation): 1996 Edition, J. Quant. Spectrosc. Radiat. Transfer, 60, 665–710, 1998. 18331

Spang, R., Riese, M., and Offermann, D.: CFC11 Measurements by CRISTA, Adv. Space Res., 19, 575–578, 1997. 18328

Steck, T.: Methods for determining regularization for atmospheric retrieval problems, Appl. Opt., 41, 1788–1797, 2002. 18331

Stiller, G. P. (Ed.): The Karlsruhe Optimized and Precise Radiative Transfer Algorithm (KOPRA), vol. FZKA 6487 of Wissenschaftliche Berichte, Forschungszentrum Karlsruhe, 2000. 18331

Stiller, G. P., von Clarmann, T., Funke, B., Glatthor, N., Hase, F., Höpfner, M., and Linden, A.: Sensitivity of trace gas abundances retrievals from infrared limb emission spectra to simplifying approximations in radiative transfer modelling, J. Quant. Spectrosc. Radiat. Transfer, 72, 249–280, 2002. 18331

Stiller, G. P., von Clarmann, T., Haenel, F., Funke, B., Glatthor, N., Grabowski, U., Kellmann, S., Kiefer, M., Linden, A., Lossow, S., and López-Puertas, M.: Observed temporal evolution of global mean age of stratospheric air for the 2002 to 2010 period, Atmos. Chem. Phys., 12, 3311–3331, doi:10.5194/acp-12-3311-2012, 2012. 18338, 18339, 18341, 18342, 18343

Thompson, T. M., Butler, J. H., Daube, B. C., Dutton, G. S., Elkins, J. W., Hall, B. D., Hurst, D. F., King, D. B., Kline, E. S., Lafleur, B. G., Lind, J., Lovitz, S., Mondeel, D. J., Montzka, S. A., Moore, F. L., Nance, J. D., Neu, J. L., Romashkin, P. A., Scheffer, A., and Snible, W. J.: Halocarbons and other atmospheric trace species, in: Summary Rep. 27 2002–2003, edited by Schnell, R. C., pp. 115–135, Clim. Monit. Diagn. Lab., Dep. of Commer., Boulder, CO, USA, 2004. 18340

Tikhonov, A.: On the solution of incorrectly stated problems and method of regularization, Dokl. Akad. Nauk. SSSR, 151, 501–504, 1963. 18331

Toon, G. C., Farmer, C. B., Shaper, P. W., Lowes, L. L., Norton, R. H., Schoeberl, M. R., Lait, L. R., and Newman, P. A.: Evidence for subsidence in the 1989 Arctic winter stratosphere from airborne infrared composition measurements, J. Geophys. Res., 97, 7963–7970, 1992. 18328

Toon, G. C., Blavier, J.-F., Sen, B., and Drouin, B. J.: Atmospheric $COCl_2$ measured by solar occultation spectrometry, Geophys. Res. Lett., 28, 2835–2838, 2001. 18332

Varanasi, P.: Absorption Coefficients of CFC-11 and CFC-12 needed for Atmospheric Remote Sensing and Global Warming Studies, J. Quant. Spectrosc. Radiat. Transfer, 48, 205–219, 1992. 18331

Varanasi, P. and Nemtchinov, V.: Thermal Infrared Absorption Coefficients of CFC-12 at Atmospheric Conditions, J. Quant. Spectrosc. Radiat. Transfer, 51, 679–687, 1994. 18331

Volk, C. M., Elkins, J. W., Fahey, D. W., Dutton, G. S., Gilligan, J. M., Loewenstein, M., Podolske, J. R., Chan, K. R., and Gunson, M. R.: Evaluation of source gas lifetimes from stratospheric observations, J. Geophys. Res., 102, 25543–25564, doi:10.1029/97JD02215, 1997. 18338

von Clarmann, T., Grabowski, U., and Kiefer, M.: On the role of non-random errors in inverse problems in radiative transfer and other applications, J. Quant. Spectrosc. Radiat. Transfer, 71, 39–46, 2001. 18339

von Clarmann, T., Ceccherini, S., Doicu, A., Dudhia, A., Funke, B., Grabowski, U., Hilgers, S., Jay, V., Linden, A., López-Puertas, M., Martín-Torres, F.-J., Payne, V., Reburn, J., Ridolfi, M., Schreier, F., Schwarz, G., Siddans, R., and Steck, T.: A blind test retrieval experiment for infrared limb emission spectrometry, J. Geophys. Res., 108, 4746, doi:10.1029/2003JD003835, 2003a. 18330

von Clarmann, T., Glatthor, N., Grabowski, U., Höpfner, M., Kellmann, S., Kiefer, M., Linden, A., Mengistu Tsidu, G., Milz, M., Steck, T., Stiller, G. P., Wang, D. Y., Fischer, H., Funke, B., Gil-López, S., and López-Puertas, M.: Retrieval of temperature and tangent altitude pointing from limb emission spectra recorded from space by the Michelson Interferometer for Passive Atmospheric Sounding (MIPAS), J. Geophys. Res., 108, 4736, doi:10.1029/2003JD003602, 2003b. 18330, 18332, 18333

von Clarmann, T., De Clercq, C., Ridolfi, M., Höpfner, M., and Lambert, J.-C.: The horizontal resolution of MIPAS, Atmos. Meas. Tech., 2, 47–54, doi:10.5194/amt-2-47-2009, 2009a. 18334

von Clarmann, T., Höpfner, M., Kellmann, S., Linden, A., Chauhan, S., Funke, B., Grabowski, U., Glatthor, N., Kiefer, M., Schieferdecker, T., Stiller, G. P., and Versick, S.: Retrieval of temperature, H_2O, O_3, HNO_3, CH_4, N_2O, $ClONO_2$ and ClO from MIPAS reduced resolution nominal mode limb emission measurements, Atmos. Meas. Tech., 2, 159–175, doi:10.5194/amt-2-159-2009, 2009b. 18332

von Clarmann, T., Stiller, G., Grabowski, U., Eckert, E., and Orphal, J.: Technical Note: Trend estimation from irregularly sampled, correlated data, Atmos. Chem. Phys., 10, 6737–6747, doi:10.5194/acp-10-6737-2010, 2010. 18339

von Clarmann, T., Funke, B., Glatthor, N., Kellmann, S., Kiefer, M., Kirner, O., Sinnhuber, B.-M., and Stiller, G. P.: The MIPAS HOCl climatology, Atmos. Chem. Phys., 12, 1965–1977, doi:10.5194/acp-12-1965-2012, 2012. 18336

Waugh, D. W., Plumb, R. A., Elkins, J. W., Fahey, D. W., Boering, K. A., Dutton, G. S., Volk, C. M., Keim, E., Gao, R.-S., Daube, B. C., Wofsy, S. C., Loewenstein, M., Podolske, J. R., Chan, K. R., Proffitt, M. H., Kelly, K. K., Newman, P. A., and Lait, L. R.: Mixing of polar votex air into middle latitudes as revealed by tracer–tracer scatterplots, J. Geophys. Res., 102, 13119–13134, 1997. 18328

Williams, W. J., Kosters, J. J., Goldman, A., and Murcray, D. G.: Measurements of stratospheric halocarbon distributions using infrared techniques, Geophys. Res. Lett., 3, 379–382, 1976. 18328

Zander, R., Rinsland, C. P., Farmer, C. B., and Norton, R. H.: Infrared spectroscopic measurements of halogenated source gases in the stratosphere with the ATMOS instrument, J. Geophys. Res., 92, 9836–9850, 1987. 18328

Table 1. Scan sequences for MIPAS FR and RR measurements (Dudhia, 2012). The RR-Nominal mode heights are latitude dependent.

Measurement mode	FR-Nominal	RR-Nominal
Version acronym	V3O	V5R
Horizontal spacing	510 km	410 km
Optical path difference	20 cm	8 cm
Spectral resolution	full:	reduced:
apodized	0.05 cm^{-1}	0.121 cm^{-1}
Sweeps/scans	17	27
Scan no. 1	68 km	70 km
Scan no. 2	60 km	66 km
Scan no. 3	52 km	62 km
Scan no. 4	47 km	58 km
Scan no. 5	42 km	54 km
Scan no. 6	39 km	50 km
Scan no. 7	36 km	46 km
Scan no. 8	33 km	43 km
Scan no. 9	30 km	40 km
Scan no. 10	27 km	37 km
Scan no. 11	24 km	34 km
Scan no. 12	21 km	31 km
Scan no. 13	18 km	29 km
Scan no. 14	15 km	27 km
Scan no. 15	12 km	25 km
Scan no. 16	9 km	23 km
Scan no. 17	6 km	21 km
Scan no. 18		19.5 km
Scan no. 19		18 km
Scan no. 20		16.5 km
Scan no. 21		15 km
Scan no. 22		13.5 km
Scan no. 23		12 km
Scan no. 24		10.5 km
Scan no. 25		9 km
Scan no. 26		7.5 km
Scan no. 27		6 km
Average number of geolocations per orbit	~74	~96

Table 2. Error budget of a V3O_CFC11_10 (FR nominal mode) retrieval from spectra recorded at 63° S, 164° E on 21 May 2003 at 22:51 UTC, for selected altitudes. The errors are given in units of pptv (%). The total error is the sum of measurement noise and parameter error. The parameter error is the sum of uncertainties in interfering species and instrumental properties, which interact as random error sources (PAN, NH_3, ..., OCS).

V3O CFC-11 Height	Total Error	Measurement Noise	Parameter Error	PAN	NH_3	Line Of Sight	Gain	Temperature	OCS
30 km	1.9 (28.4)	1.8 (26.9)	0.4 (6.7)	0.3 (4.2)	0.1 (1.8)	0.3 (4.6)	<0.1 (<0.1)	<0.1 (0.5)	0.1 (0.9)
25 km	6.4 (17.4)	6.1 (16.6)	1.9 (5.2)	0.6 (1.7)	0.6 (1.6)	1.6 (4.4)	0.2 (0.5)	0.2 (0.6)	0.3 (0.9)
20 km	8.0 (12.7)	5.9 (9.4)	5.5 (8.8)	1.4 (2.2)	0.6 (0.9)	5.2 (8.3)	0.7 (1.1)	0.4 (0.7)	0.5 (0.8)
15 km	9.3 (4.9)	2.8 (1.5)	8.8 (4.7)	5.0 (2.6)	1.8 (1.0)	6.8 (3.6)	1.4 (0.7)	1.0 (0.5)	0.9 (0.5)
10 km	45.0 (15.7)	4.0 (1.4)	44.0 (15.3)	44.0 (15.3)	1.9 (0.7)	4.2 (1.5)	0.1 (<0.1)	0.4 (0.1)	1.3 (0.5)

Table 3. Error budget of a V5R_CFC11_220 (RR nominal mode) retrieval from spectra recorded at 37° N, 29° W on 19 September 2009 at 00:11 UTC for selected altitudes. The errors are given in units of pptv (%). Details as for Table 2.

V5R CFC-11 Height	Total Error	Measurement Noise	Parameter Error	PAN	NH_3	Line Of Sight	Gain	Temperature	OCS
30 km	1.9 (35.2)	1.7 (31.5)	0.7 (12.6)	0.6 (10.9)	0.1 (1.4)	0.3 (5.9)	0.1 (1.6)	<0.1 (0.3)	<0.1 (0.4)
25 km	6.1 (14.8)	5.5 (13.3)	2.6 (6.3)	1.1 (2.7)	<0.1 (0.1)	2.3 (5.6)	0.1 (0.2)	0.1 (0.2)	0.1 (0.3)
20 km	9.8 (6.7)	5.5 (3.7)	8.2 (5.6)	1.1 (0.7)	0.2 (0.2)	8.0 (5.4)	1.4 (1.0)	0.3 (0.2)	0.2 (0.1)
15 km	11.0 (4.4)	4.8 (1.9)	9.3 (3.7)	0.9 (0.4)	0.6 (0.3)	8.7 (3.5)	3.1 (1.2)	0.5 (0.2)	0.3 (0.1)
10 km	19.0 (7.7)	4.5 (1.8)	18.0 (7.3)	8.6 (3.5)	2.3 (0.9)	15.0 (6.1)	5.8 (2.4)	1.0 (0.4)	0.8 (0.3)

Table 4. Horizontal information smearing (full width at half maximum of the horizontal component of the 2-D averaging kernel) for CFC-11.

Mode Spectr. Resol.	Nominal full	Nominal reduced
25 km	440 km	468 km
20 km	335 km	497 km
15 km	293 km	159 km
10 km	199 km	295 km

Table 5. Information displacement for CFC-11 retrievals. Negative distances are displacement towards beyond the tangent point, positive distances are displacement towards the satellite.

Mode Spectr. Resol.	Nominal full	Nominal reduced
25 km	561 km	249 km
20 km	112 km	82 km
15 km	−74 km	105 km
10 km	−146 km	4 km

Table 6. Error budget of a V3O_CFC12_10 (FR nominal mode) retrieval from spectra recorded at 63° S, 164° E on 21 May 2003 at 22:51 UTC for selected altitudes. The errors are given in units of pptv (%). Details as for Table 2.

V3O CFC-12 Height	Total Error	Measurement Noise	Parameter Error	Line Of Sight	Gain	Temp. Inhomog.	Temp.	NH_3
35 km	21.0 (87.6)	21.0 (87.6)	1.6 (6.7)	0.7 (2.9)	1.2 (5.0)	0.5 (1.9)	0.6 (2.7)	<0.1 (0.1)
30 km	20.0 (58.6)	20.0 (58.6)	3.1 (9.1)	3.0 (8.8)	0.3 (0.9)	0.2 (0.6)	0.1 (0.4)	0.1 (0.2)
25 km	20.0 (13.2)	18.0 (11.9)	8.6 (5.7)	8.4 (5.5)	1.0 (0.6)	<0.1 (<0.1)	1.1 (0.7)	<0.1 (<0.1)
20 km	20.0 (7.4)	15.0 (5.5)	13.0 (4.8)	13.0 (4.8)	3.4 (1.3)	0.6 (0.2)	2.1 (0.8)	0.2 (0.1)
15 km	18.0 (3.8)	9.4 (2.0)	15.0 (3.1)	15.0 (3.1)	3.5 (0.7)	0.4 (0.1)	2.7 (0.6)	0.8 (0.2)
10 km	18.0 (2.5)	12.0 (1.7)	13.0 (1.8)	8.0 (1.1)	4.5 (0.6)	2.6 (0.4)	1.5 (0.2)	8.8 (1.2)

Table 7. Error budget of a V5R_CFC12_220 (RR nominal mode) retrieval from spectra recorded at 37° N, 29° W on 19 September 2009 at 00:11 UTC, for selected altitudes. The errors are given in units of pptv (%). Details as for Table 2.

V5R CFC-12 Height	Total Error	Measurement Noise	Parameter Error	Line Of Sight	Gain	Temp.	Shift	NH_3
35 km	28.0 (32.1)	27.0 (31.0)	6.7 (7.7)	6.3 (7.2)	2.1 (2.4)	0.5 (0.6)	0.4 (0.4)	0.1 (0.1)
30 km	24.0 (22.9)	22.0 (21.0)	8.8 (8.4)	8.4 (8.0)	2.5 (2.4)	0.6 (0.6)	0.3 (0.3)	0.1 (0.1)
25 km	22.0 (9.0)	21.0 (8.6)	5.1 (2.1)	4.2 (1.7)	2.9 (1.2)	0.7 (0.3)	0.2 (0.1)	<0.1 (<0.1)
20 km	22.0 (5.3)	16.0 (3.9)	15.0 (3.6)	14.0 (3.4)	5.1 (1.2)	1.2 (0.3)	0.1 (<0.1)	<0.1 (<0.1)
15 km	22.0 (4.1)	15.0 (2.8)	16.0 (3.0)	13.0 (2.4)	9.3 (1.7)	1.7 (0.3)	0.1 (<0.1)	0.2 (<0.1)
10 km	64.0 (12.0)	13.0 (2.4)	63.0 (11.9)	57.0 (10.7)	27.0 (5.1)	6.3 (1.2)	0.1 (<0.1)	1.3 (0.2)

Table 8. Horizontal information smearing (full width at half maximum of the horizontal component of the 2-D averaging kernel) for CFC-12.

Mode Spectr. Resol.	Nominal full	Nominal reduced
35 km	503 km	510 km
30 km	430 km	444 km
25 km	406 km	557 km
20 km	304 km	394 km
15 km	250 km	578 km
10 km	262 km	292 km

Table 9. Information displacement for CFC-12 retrievals.

Mode Spectr. Resol.	Nominal full	Nominal reduced
35 km	187 km	−19 km
30 km	153 km	13 km
25 km	−61 km	40 km
20 km	−87 km	83 km
15 km	−177 km	147 km
10 km	−373 km	−61 km

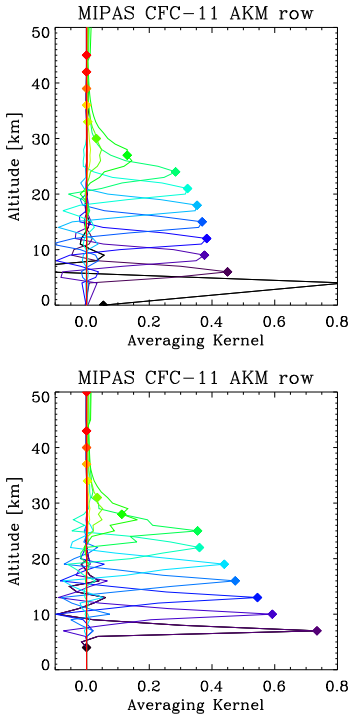

Fig. 1. Rows of averaging kernels of CFC-11 measurements for FR nominal mode (top) and RR nominal mode (bottom). Diamonds represent the nominal altitudes (i.e. the diagonal value of the averaging kernel matrix). Only every third kernel is shown.

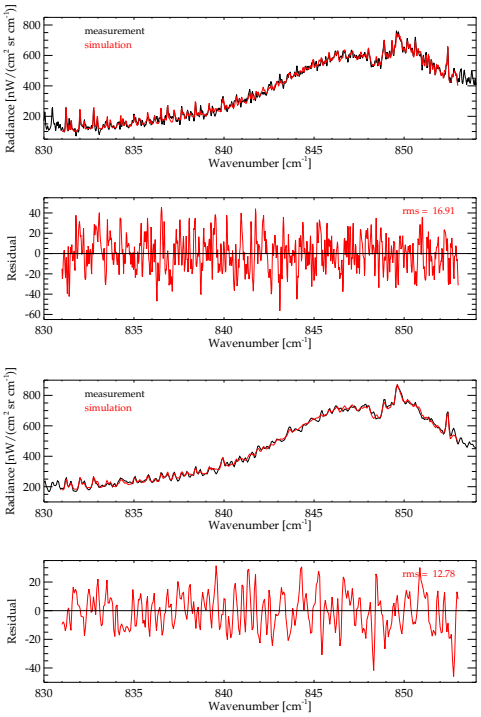

Fig. 2. Typical measured (black) and calculated (red) spectra of CFC-11 and the fit residual in 14 km in the 831 and 853 cm^{-1} spectral region for the FR (top) and the RR (bottom) nominal measurement modes.

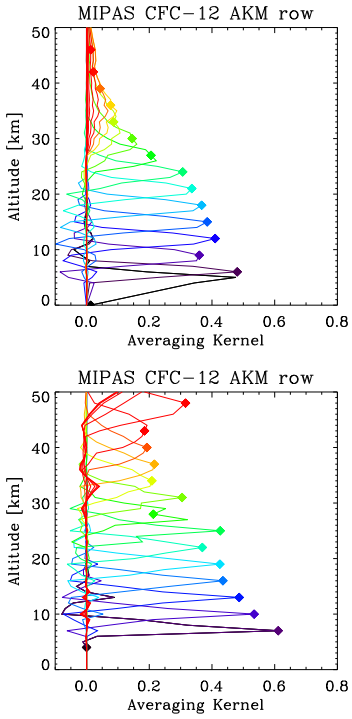

Fig. 3. Rows of averaging kernels of CFC-12 measurements for FR nominal mode (top) and RR (bottom) nominal measurement modes. Diamonds represent the nominal altitudes (i.e. the diagonal value of the averaging kernel matrix). Only every third kernel is shown.

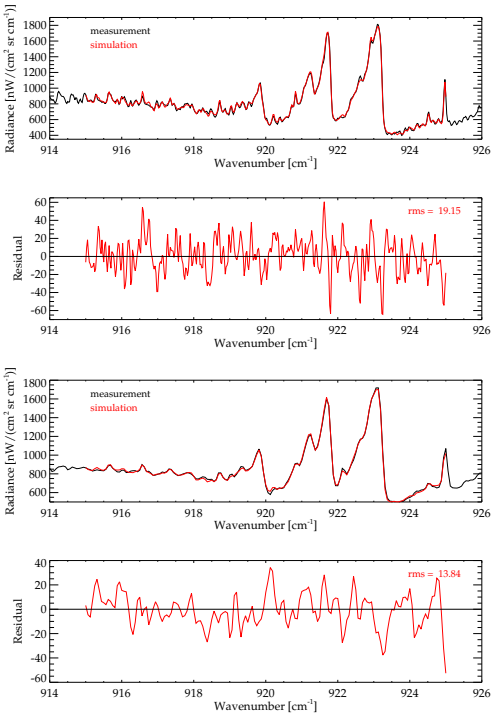

Fig. 4. Typical measured (black) and calculated (in red) spectra of CFC-12 and the fit residual in 11 km in the 915.0–925.0 cm^{-1} spectral region for the FR (top) and the RR (bottom) spectral resolution nominal modes.

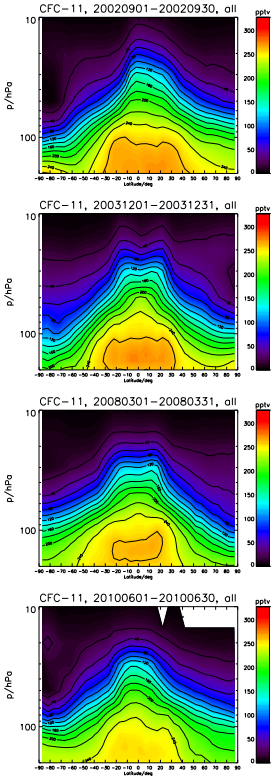

Fig. 5. CFC-11 monthly zonal mean distribution between 200 hPa and 10 hPa in September 2002, December 2003, March 2008, and June 2010.

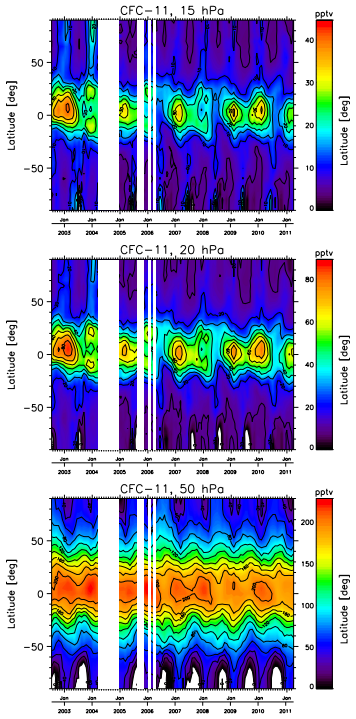

Fig. 6. Time series of CFC-11 as a function of latitude between July 2002 and April 2011 in 15 hPa, 20 hPa and 50 hPa. Note there is no MIPAS data available between April and December 2004. The white spots in the southern polar region indicate data gaps due to the existence of not detected polar stratospheric clouds, because no retrievals are possible below cloud top altitude.

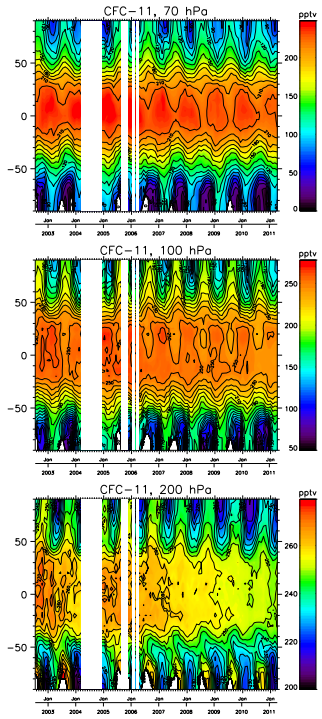

Fig. 7. Time series of CFC-11 as a function of latitude between July 2002 and April 2011 in 70 hPa, 100 hPa and 200 hPa. The increased CFC values in the southern polar regions at 200 hPa are not reliable and indicate not detected clouds.

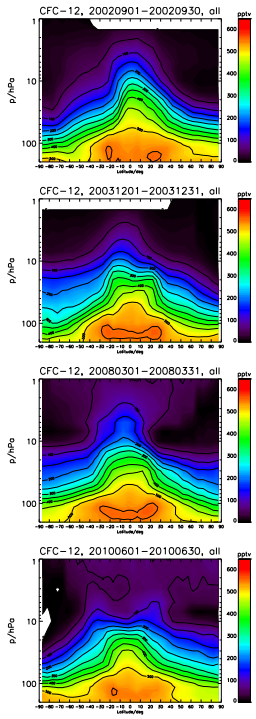

Fig. 8. CFC-12 monthly zonal mean distribution between 200 hPa and 1 hPa in September 2002, December 2003, March 2008, and June 2010.

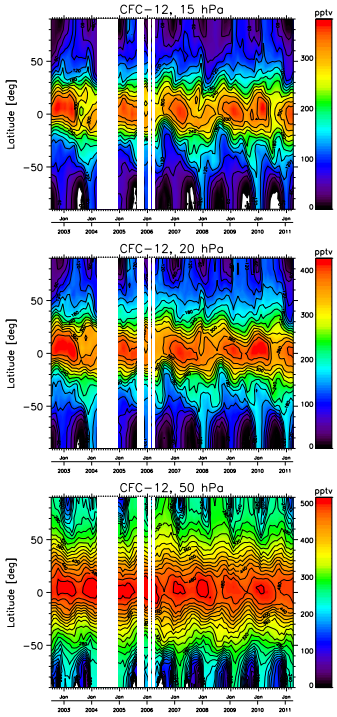

Fig. 9. Time series of CFC-12 as a function of latitude between July 2002 and April 2011 at 15 hPa, 20 hPa and 50 hPa. Details as for Fig. 6.

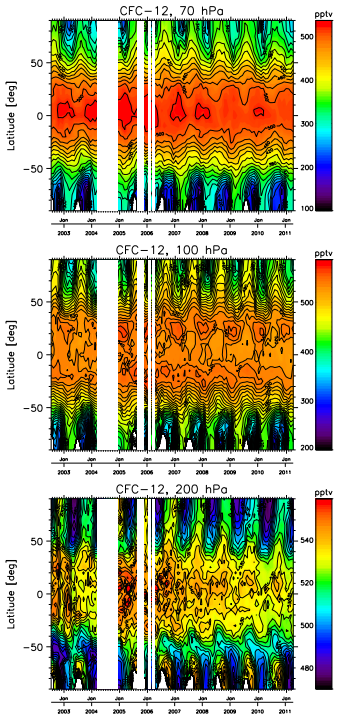

Fig. 10. Time series of CFC-12 as a function of latitude between July 2002 and April 2011 at 70 hPa, 100 hPa and 200 hPa. Details as for Fig. 7.

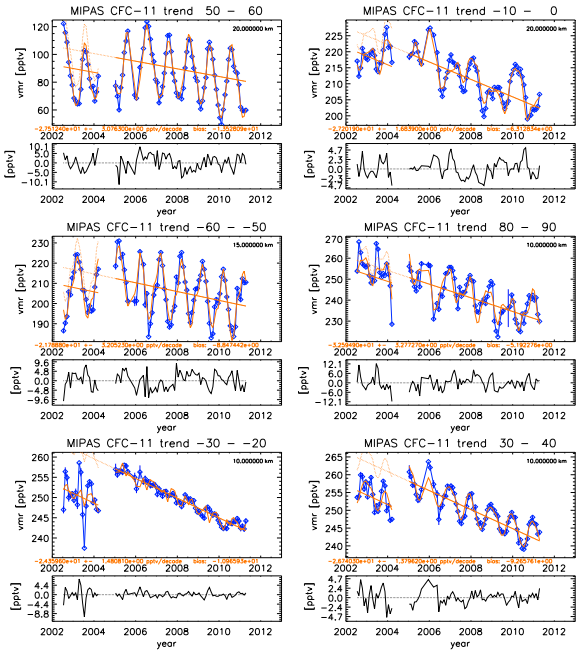

Fig. 11. Temporal evolution of CFC-11 for northern mid-latitudes (50° N to 60° N) at 20 km (top left panel), inner tropics (0° S to 10° S) at 20 km (top right panel), southern mid-latitudes (50° S to 60° S) at 15 km altitude (middle left panel), northern polar latitudes (80° N to 90° N) at 10 km altitude (middle right panel), southern subtropics (20° S to 30° S) at 10 km altitude (lower right panel), and northern mid-latitudes (30° N to 40° N) at 10 km (lower right panel), The blue diamonds are the MIPAS data points; the bold solid orange curve is the fit through the data. The linear part of the regression represented by the straight orange line. The dotted orange curve and straight line are the respective bias-corrected fit and its linear component, respectively. In the lower part of each panel, the residuals between MIPAS CFC-11 monthly zonal means and the trend-corrected regression function are shown. The trend of CFC-11 in pptv per decade, its uncertainty, and the bias between the data subsets V3O_CFC11_10 and V5R_CFC11_220 are printed in orange font.

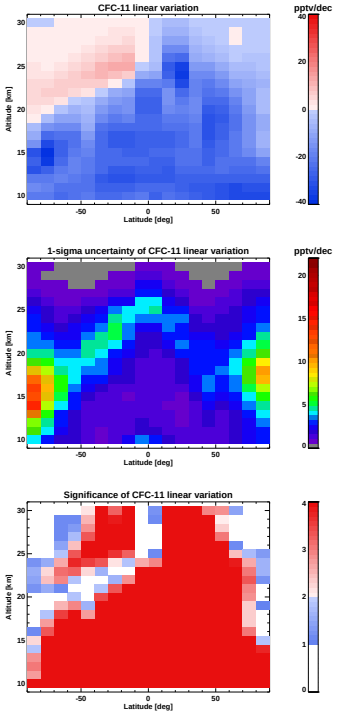

Fig. 12. CFC-11 trends over the years 2002 to 2011 as a function of altitude and latitude in pptv per decade (top); 1-sigma trend uncertainties (middle); and significance of the trend in terms of multiples of sigma (bottom).

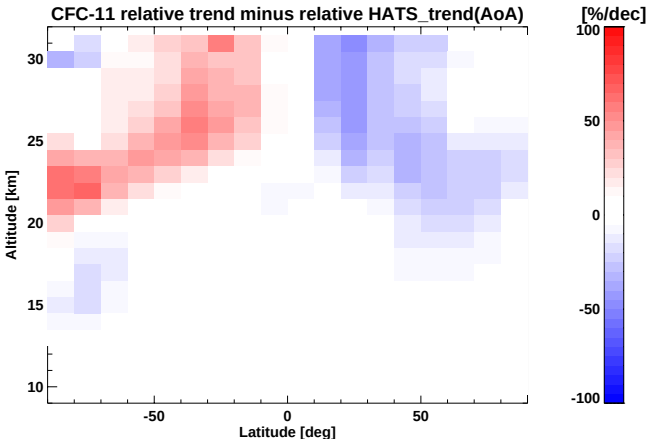

Fig. 13. Differences of relative trends between MIPAS and HATS data under consideration of the age of air over the years 2002 to 2011 as a function of altitude and latitude in % per decade for CFC-11.

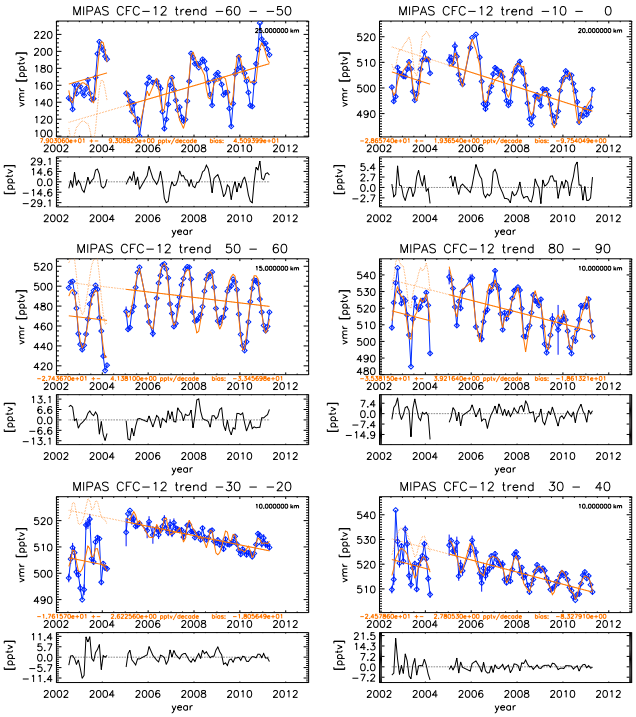

Fig. 14. Temporal evolution of CFC-12 for southern mid-latitudes (50° S to 60° S) at 25 km (top left panel), inner tropics (0° S to 10° S) at 20 km (top right panel), northern mid-latitudes (50° N to 60° N) at 15 km altitude (middle left panel), and northern polar latitudes (80° N to 90° N) at 10 km altitude (middle right panel) southern subtropics (20° S to 30° S) at 10 km altitude (lower right panel), and northern mid-latitudes (30° N to 40° N) at 10 km (lower right panel). Details as for Fig. 11.

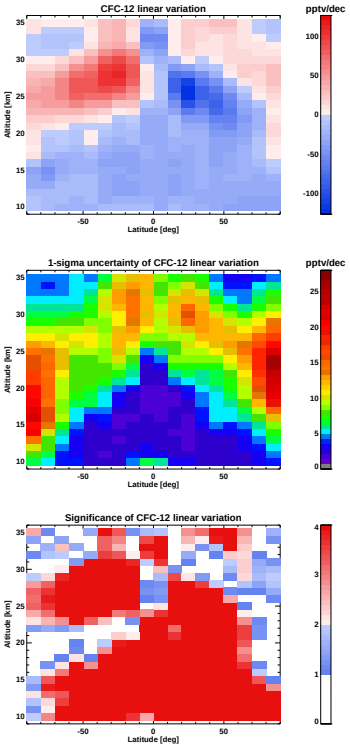

Fig. 15. CFC-12 trends over the years 2002 to 2011 as a function of altitude and latitude in pptv per decade (top); 1-sigma trend uncertainties (middle); and significance of the trend in terms of multiples of sigma (bottom).

Discussion Paper | Discussion Paper | Discussion Paper | Discussion Paper |

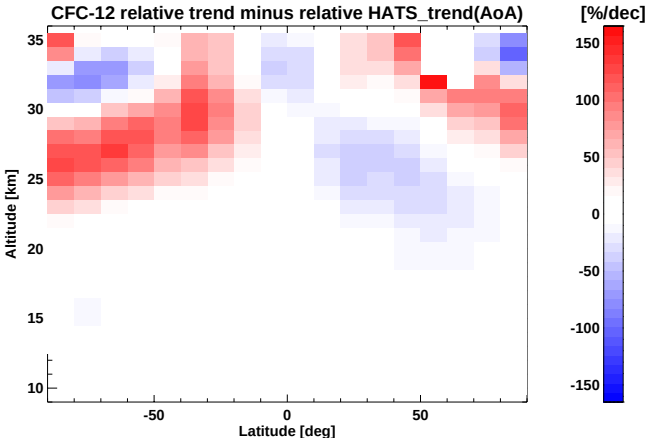

Fig. 16. As for Fig. 13 but for CFC-12.